HNO_3. Solution scavanged with I_2 in benzene, then Zr, Nb, and Pa extracted into benzene, 0.4f in TTA. Benzene phase ignited; resulting ZrO_2 solid mounted.

Same activities detected as in the zirconium fraction. As the ratios of the different activities detected were the same within experimental error as those found in the zirconium samples, it was concluded that protactinium was quantitatively carried in both procedures. The method of isolating Pa alone with Zr by two independent chemical procedures was adopted in order to determine the chemical yield without the necessity of adding Pa^{231} tracer.

PHYSICAL REVIEW VOLUME 88, NUMBER 4 NOVEMBER 15, 1952

Grain Boundary Barriers in Germanium*

W. E. TAYLOR,† N. H. ODELL,‡ AND H. Y. FAN
Purdue University, Lafayette, Indiana

(Received July 21, 1952)

High resistance at crystal grain boundaries in n-type germanium is investigated. The resistance is symmetrical with respect to the direct on of the current and resembles the characteristics of a rectifier in the blocking direction. Such barriers are also photosensitive. The barrier is eliminated when the material is converted to p-type by nucleon bombardment or heat treatment. A theory is developed assuming the existence of surface states at the boundary. The ability of the barriers to withstand high voltages, around 100 volts, is explained by showing that the surface charge increases with increasing voltage. The dc conductance of the barrier, measured at different temperatures, agrees with theory in the dependence on temperature as well as in the order of magnitude. At sufficiently low temperatures the barriers show a capacitance independent of the frequency, whereas at higher temperatures the barrier admittance is strongly frequency dependent. These results are in agreement with the theory, showing that at low temperatures the current across the boundary is mainly carried by electrons, the hole current becoming increasingly important as the temperature is raised. The height of the potential barrier above the Fermi level is determined and found to be independent of temperature. A small difference in the measured breakdown voltage for the two directions of current is attributed to a difference in impurity concentration on the two sides of the boundary, which is confirmed by the ac measurements. The number of electrons on the boundary states is found to be of the order 10^{12} cm^{-2} at the breakdown, which may be the saturation of the boundary states. However, the field at breakdown is only a few times lower than the critical value for the onset of the Zener current, and this mechanism cannot be definitely ruled out.

INTRODUCTION

GRAIN boundaries in n-type germanium are often found to present a high resistance to current flow in either direction.[1–4] Curve A, Fig. 1, shows the potential variation as measured by a whisker probe along a germanium sample with a grain boundary. The potential is seen to make an abrupt jump at the boundary, corresponding to 95 percent of the total potential difference applied to the sample. This high boundary resistance is not due to an insulating layer of foreign material. Microphotographs do not reveal any second phase at such boundaries. Furthermore, when a sample with a high resistance grain boundary is changed into p-type, either by nucleon irradiation[5] (curve B, Fig. 1) or by heating to high temperatures and subsequent quenching,[2] the boundary resistance vanishes. It reappears when the sample is changed back to n-type by annealing.

The resistance of the boundary is nonohmic, increasing with increasing voltage, and is approximately symmetrical regarding the direction of current. Figure 2 shows a set of typical current-voltage curves. The curve for both directions of current flow resembles the ordinary rectifier characteristic in the blocking direction. Furthermore, the grain boundary is also photosensitive; the photovoltage generated by a sharp pencil of light reverse its sign as the light crosses the boundary, and the signs are such as to agree with the picture of two potential barriers of a n-type semiconductor existing at the boundary back to back.[6] Merritt[7] and Benzer[8] have shown that two wedge-shaped pieces of uniform n-type germanium brought to a point contact give a current-voltage characteristic similar to the curve in Fig. 2. The nonohmic contact resistance was interpreted as due to potential barriers at free surfaces of n-type

* Work supported by a Signal Corps contract. The dc measurements are part of a thesis submitted by W. E. Taylor and the ac measurements are part of a thesis submitted by N. H. Odell to the faculty of Purdue University in partial fulfillment of the requirements for the Ph.D. degree.

† Now at Motorola Research Laboratory, Phoenix, Arizona.

‡ Now at Bell Telephone Laboratories, Allentown, Pennsylvania.

[1] K. Lark-Horovitz, NDRC Report 14–585 (1945) (unpublished).

[2] G. Pearson, Phys. Rev. **76**, 459 (1949).

[3] W. E. Taylor and H. Y. Fan, Phys. Rev. **78**, 335 (1950).

[4] N. H. Odell and H. Y. Fan, Phys. Rev. **78**, 334 (1950).

[5] W. Taylor and K. Lark-Horovitz, Purdue Semiconductor Research Progress Report (October, 1948) (unpublished); reference 3.

[6] M. Becker and H. Y. Fan, Purdue Semiconductor Research Progress Report (June, 1949); see also reference 2.

[7] E. Merritt, Proc. Natl. Acad. Sci. **11**, 743 (1925).

[8] S. Benzer, Phys.Rev. **71**, 141 (1947).

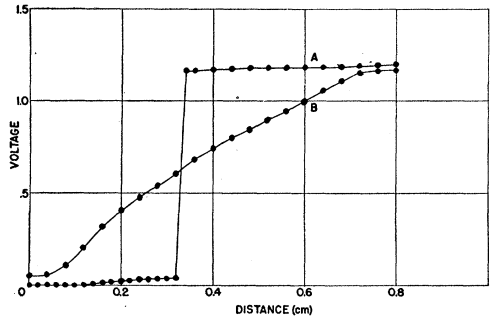

FIG. 1. Potential drop along a sample with a grain boundary. Curve A, original n-type sample. Curve B, sample converted to p-type by deuteron irradiation.

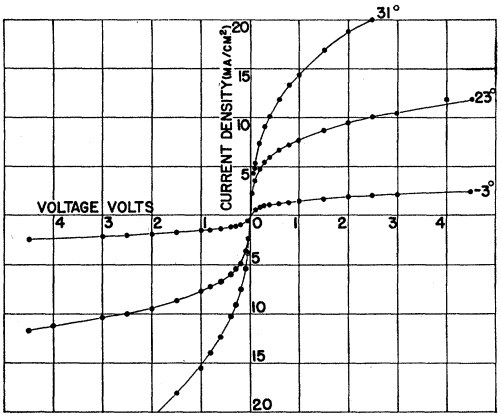

FIG. 2. Current-voltage characteristics of a grain boundary at different temperatures.

germanium due to surface states postulated by Bardeen.[9] Thus the similar behavior of grain boundaries can be due likewise to the existence of surface states at the boundary.

Surface states at the boundary may be produced either by the lattice misfits or by a segregation of acceptor impurities. The specimens studied were obtained from germanium melts, in which the resistivity indicates that the parts solidified last contain more n-type or less p-type impurities. The grain boundaries were formed as two separate crystals joined together in their growth. Although it does not provide a conclusive proof, this observation seems to be against the segregation of p-type impurities at the grain boundaries in these melts. In the following we shall first give a theoretical treatment of the problem on the basis of the existence of boundary states. Then the experimental results will be presented and discussed in the light of the theory. The theory is independent of the cause of the boundary states. However, if near the boundary there is an extensive region with excess acceptor impurities, then the problem could be treated by the same method used for n–p–n junctions.[10] As we shall see, the experimental evidence is against such an interpretation.

[9] J. Bardeen, Phys. Rev. **71**, 717 (1947).
[10] Shockley, Sparks, and Teal, Phys. Rev. **83**, 151 (1950).

THEORY

The electron energy level diagram according to our picture is shown in Fig. 3. Figure 3a corresponds to equilibrium condition, while Fig. 3b is drawn for the condition under an applied voltage V_a. Localized boundary states are assumed with energy levels in the forbidden gap. Under equilibrium some of these states, i.e., roughly those below the Fermi level, are occupied by electrons, giving rise to a negative surface charge q. A space charge region constituting a potential barrier results on either side of the boundary. The sum of the positive space charges is equal to q in magnitude. When the specimen is converted to p-type, either by nucleon bombardment or by heat treatment, the Fermi level is shifted close to the bottom of the energy gap. Most of the boundary states will not be occupied by electrons, and there will no longer be appreciable potential barriers. The high resistance of the boundary is thereby eliminated.

Impurities in germanium usually have very small activation energies and are practically completely ionized even in the bulk material, except at very low temperatures. Thus the space charge density in the potential barriers is equal to the impurity concentration N, if the space charges of the carriers are neglected. These are easily seen to be small compared to the space charge of impurities, provided the top of the valence band does not come too close to the Fermi level at the boundary, in which case the hole concentration at the boundary may be too high for its space charge to be neglected. However, such a situation, if it exists, is limited to a small part of the barriers. We shall overlook this possible complication and deal with fixed space charge of impurity ions. Solution of the Poisson equation gives for the potential drop across such a barrier:

$$V=\kappa E^2/8\pi eN=2\pi eNl^2/\kappa. \tag{1}$$

The total space charge in the barrier is

$$Q=eNl=(\kappa eNV/2\pi)^{\frac{1}{2}}, \tag{2}$$

where κ is the dielectric constant of the medium, E is the electric field at the top of the barrier, and l is the barrier thickness.

Referring to Fig. 3 we shall take the direction from left to right as positive. The potential difference across the boundary is

$$V_1-V_2=\frac{\kappa}{8\pi e}\left(\frac{E_1^2}{N_1}-\frac{E_2^2}{N_2}\right), \tag{3}$$

and the surface charge on the boundary states is

$$q=-(\kappa e/2\pi)^{\frac{1}{2}}[(N_1V_1)^{\frac{1}{2}}+(N_2V_2)^{\frac{1}{2}}]$$
$$=-(\kappa/4\pi)(E_1-E_2). \tag{4}$$

We shall see later that the experimental results show some dissymmetry between the two sides of the boundary, which is attributable to a small difference between N_1 and N_2. However, this difference is of no significant importance in some of the following discussions. For simplicity we shall assume $N_1=N_2=N$, except when we want to deal specifically with the unsymmetrical behavior. Thus, under equilibrium,

$$\phi_1=\phi_2=\phi; \quad V_{10}=V_{20}=\phi/e; \qquad E_{10}=-E_{20}=-2\pi q_0/\kappa. \tag{5}$$

Under an applied voltage across the barrier,

$$V_a=V_1-V_2, \tag{6}$$

we get from (3) and (4):

$$E_1=-2\pi q/\kappa-eNV_a/q, \quad E_2=2\pi q/\kappa-eNV_a/q. \tag{7}$$

Substituting in (1), we find

$$V_1=(\kappa/8\pi eN)(2\pi q/\kappa+eNV_a/q)^2, \qquad V_2=(\kappa/8\pi eN)(2\pi q/\kappa-eNV_a/q)^2. \tag{8}$$

E_2 and V_2 reduce to zero if V_a reaches the critical value,

$$V_c=(2\pi/\kappa eN)q^2. \tag{9}$$

If q remains equal to q_0 we find, in view of (5),

$$V_c=4\phi. \tag{10}$$

Thus the maximum voltage drop across the grain boundary is 4ϕ, where ϕ is only a fraction of 1 ev. Actually grain boundaries present a very high resistance for voltages up to 100 volts. This fact can be understood in the following way. We shall show shortly that, with increasing applied voltage, the electron concentration at the boundary surface increases whereas the hole concentration decreases. Consequently, the number of electrons on the boundary states will be increased due to the processes tending to establish equilibrium electron distribution among the boundary states, the conduction band, and the valence band. The increase of the negative charge on the boundary reduces the decrease of V_2 and shifts more of the applied voltage to the increase of V_1. Putting $V_2=V_{20}=\phi$ or $E_2=E_{20}$, we find by using (5),

$$2\pi q/\kappa-eNV_a/q=2\pi q_0/\kappa, \qquad q=(q_0/2)[1+(1+V_a/\phi)^{\frac{1}{2}}]. \tag{11}$$

Thus if q could follow the increase of V_a according to (11), then V_2 will remain constant and $V_1=V_{10}+V_a$. We shall not attempt to derive the actual relationship between q and V_a, which requires detailed knowledge of electron transition processes between the various energy levels. The fact that the grain boundary stands voltages as high as 100 volts, while the change of V_2 must be less than ϕ, shows that (11) is nearly fulfilled. There is a limit q_m corresponding to the total number of the boundary states. Equation (9) then sets an upper limit for the voltage drop across the grain boundary. When this voltage is reached, the current will increase very steeply with little increase in V_a; the grain boundary barrier breaks down.

Direct-Current Conductance

To derive the current-voltage relationship, we shall consider the barriers on the two sides of the boundary separately and join the solutions by the condition of current continuity. We assume that the electron-hole recombinations within the barriers and at the boundary surface do not contribute appreciably to the current. The electron and hole currents should then be constant separately throughout the composite barrier. According to Schottky's diffusion theory for barriers, the current density of either type of carriers is given approximately by

$$i=e\mu E[n_B-n_A\exp(\mp eV_{AB}/kT)]/[1-\exp(\mp eV_{AB}/kT)], \tag{12}$$

where μ is the carrier mobility, E is the field at the top of the barrier, the subscript A refers to the bottom of the barrier, and the subscript B refers to the top of the barrier. The negative and the positive signs should be taken for electron current and hole current, respectively. For barriers in an n-type semiconductor we should have $eV_{AB}\gg kT$. Furthermore, the concentration of electrons at A is equal to the bulk concentration n_{e0}. Thus we can write

$$i_e=e\mu_e E[n_{eB}-n_{e0}\exp(-eV_{AB}/kT)]. \tag{13}$$

For simplicity we shall assume that the bulk properties, and therefore n_{e0}, are the same on the two sides of the

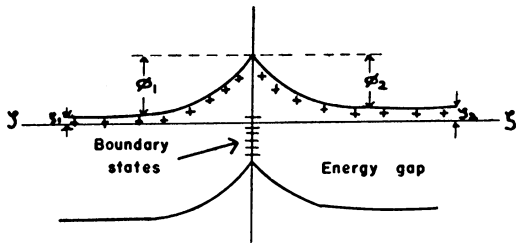

FIG. 3a. Energy level diagram for a grain boundary at equilibrium.

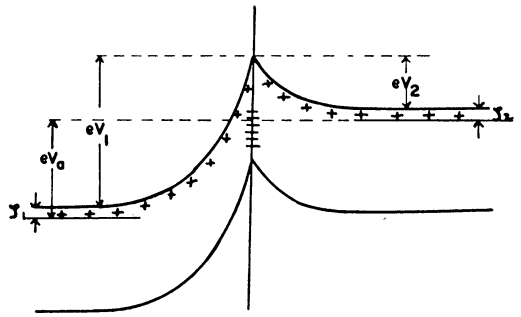

FIG. 3b. Energy level diagram for a grain boundary under applied voltage V_a.

boundary. Equating i_e for the two sides, we get

$$n_{eB}(E_1-E_2)=n_{e0}[E_1\exp(-eV_1/kT) -E_2(-eV_2/kT)]. \quad (14)$$

Eliminating n_B from (13) by (14), we get

$$i_e=-e\mu_e\frac{E_1E_2}{E_1-E_2}n_{e0}\exp(-eV_2/kT) \times[1-\exp(-eV_a/kT)] \quad (15)$$

for an applied voltage across the grain boundary $V_a=V_1-V_2$. It is to be remembered that $E_1>0$ and $E_2<0$ [see (5)]. The slope of (i_e, V_a) curve at $V_a=0$, where $E_1=-E_2=E_0$, follows from (15):

$$G_{e0}=(e^2/2kT)\mu_eE_0n_{e0}\exp(-e\phi/kT) =(e^2/2kT)\mu_eE_0AT^{\frac{1}{2}}\exp[-(\phi+\zeta)/kT], \quad (16)$$

where $A=2(2\pi m_ek/h^2)^{\frac{3}{2}}$ and ζ is the Fermi energy.

The hole current can be treated in the same manner as the current through a p–n junction. According to (12),

$$i_h=e\mu_hE[n_{hA}-n_{hB}\exp(-eV_{AB}/kT)], \quad (17)$$

in view of $eV_{AB}\gg kT$. The hole concentration at A is, however, not equal to n_{h0}, the equilibrium concentration in the bulk. Equating i_h for the two sides, we get

$$n_{h1}E_1-n_{h2}E_2 =n_{hB}[E_1\exp(-eV_1/kT)-E_2\exp(-eV_2/kT)], \quad (18)$$

$$i_h=e\mu_hE_1E_2\frac{n_{h2}\exp(-eV_1/kT)-n_{h1}\exp(-eV_2/kT)}{E_1\exp(-eV_1/kT)-E_2\exp(-eV_2/kT)}. \quad (19)$$

The values n_{h1} and n_{h2} are determined by the continuity of i_h at the junctions between the barriers and the bulk semiconductor. Since $n_h\ll n_e$ in the bulk semiconductor, the hole current due to the field, which acts on electrons as well as holes, must be negligible. Appreciable hole current can be due only to diffusion as the result of a gradient in the concentration of holes:

$$i_h=-eD_hdn_h/dx. \quad (20)$$

For steady current,

$$\frac{\partial n_h}{\partial t}=-\frac{1}{e}\frac{\partial i_h}{\partial x}-\frac{n_h-n_{h0}}{\tau}=0, \quad (21)$$

where n_{h0} is the equilibrium hole concentration in the semiconductor and τ is the lifetime of holes. The solution of these equations with the boundary condition $n_h=n_{h0}$ at $x=\infty$, gives for the current flowing into the semiconductor from its boundary with barrier, where $n_h=n_{hA}$,

$$i_h=e(D_h/\tau)^{\frac{1}{2}}(n_{hA}-n_{h0}). \quad (22)$$

Equating the hole current flowing into the grain boundary barrier from side 1 to that flowing out of it into side 2, we get

$$-(n_{h1}-n_{h0})=n_{h2}-n_{h0};\quad n_{h1}+n_{h2}=2n_{h0}. \quad (23)$$

Equations (19) and (22) give

$$\frac{i_h}{e}\left\{\left[\frac{1}{\mu_hE_2}-\left(\frac{\tau}{D_h}\right)^{\frac{1}{2}}\right]\exp\left(-\frac{eV_1}{kT}\right) -\left[\frac{1}{\mu_hE_1}+\left(\frac{\tau}{D_h}\right)^{\frac{1}{2}}\right]\exp\left(-\frac{eV_2}{kT}\right)\right\} =n_{h0}\left[\exp\left(-\frac{eV_1}{kT}\right)-\exp\left(-\frac{eV_2}{kT}\right)\right].$$

For germanium at room temperature $\mu_h=2000$ cm^2/volt sec, $D_h=50$ cm^2/sec, and $\tau\gtrsim 10^{-6}$ sec. Usually E is of the order 10^4 volt/cm. Thus

$$\mu_hE\gg(D_h/\tau)^{\frac{1}{2}}, \quad (24)$$

$$i_h=e(D_h/\tau)^{\frac{1}{2}}n_{h0}[1-\exp(-eV_a/kT)]/ [1+\exp(-eV_a/kT)]. \quad (25)$$

Under equilibrium conditions, $V_1=V_2$, $E_1=-E_2=E_0$, and $n_{h1}=n_{h2}=n_{h0}$. It follows from (25) that the slope of (i_h, V_a) curve at the origin is

$$G_{h0}=(e^2/2kT)(D_h/\tau)^{\frac{1}{2}}n_{h0}. \quad (26)$$

Having dealt with the current voltage relationship, we shall now show that the surface charge on the boundary actually increases with the applied voltage as stated at the end of the previous section. Consider first the electron concentration at the boundary n_{eB}. According to (14), for applied voltages $V_a\gg kT/e$,

$$n_{eB}(E_1-E_2)\approx-n_{e0}E_2\exp(-eV_2/kT).$$

In the convention adopted in the previous section, $E_1>0$ and $E_2<0$. According to (1), $|E_2|$ is proportional to $V_2^{\frac{1}{2}}$; and according to (4), (E_1-E_2) is proportional to $-q$ or the number of electrons on the boundary states. If q remains unchanged, then

$$\frac{dn_{eB}}{dV_a}\propto V_2^{\frac{1}{2}}(kT/2eV_2-1)\exp(-eV_2/kT)\frac{dV_2}{dV_a}.$$

According to (8), $(dV_2/dV_a)_q$ is negative. With $eV_2\gg kT$, the right-hand side is positive. Thus n_{eB} will increase with the applied voltage. Consider now the hole concentration at the boundary. For $V_a\gg kT/e$ we get, from

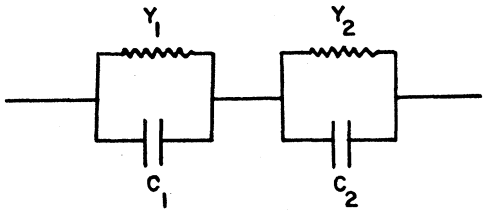

FIG. 4. Equivalent circuit for a grain boundary barrier.

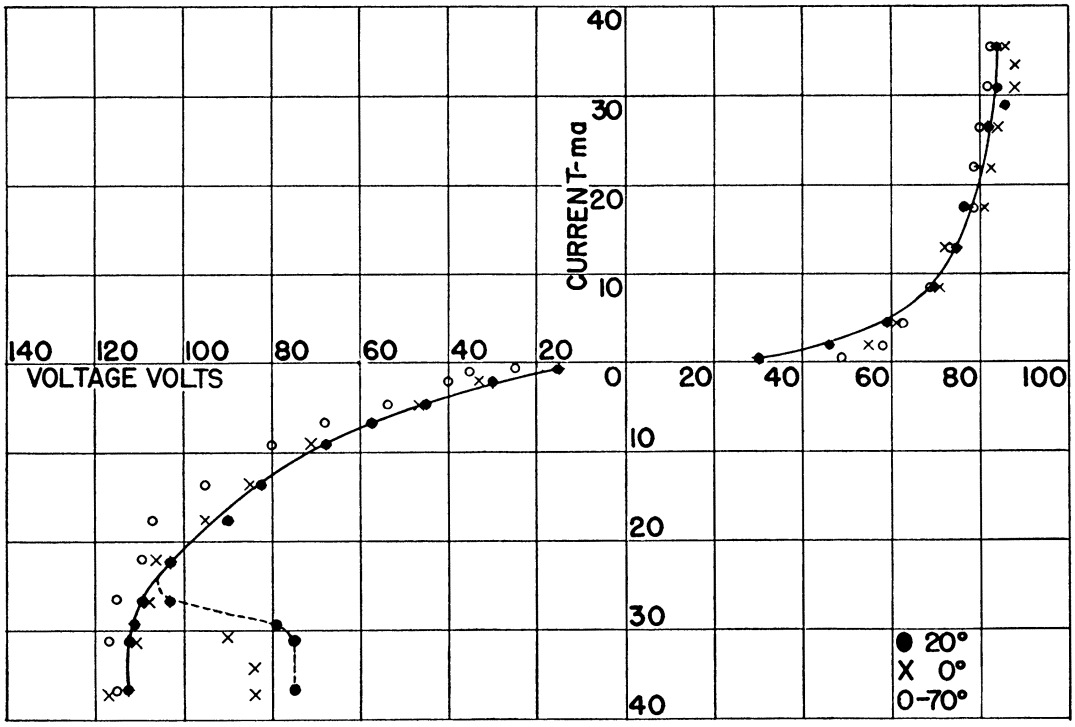

FIG. 5. Current-voltage relationship for a grain boundary at different temperatures, showing breakdown of the barrier.

(25),

$$i_h = e(D_h/\tau)^{\frac{1}{2}} n_{h0}[1-2\exp(-eV_a/kT)].$$

Comparing this expression with (22), we get for the hole concentration at the end of the grain boundary barrier on side 1:

$$n_{h1} = 2n_{h0}\exp(-eV_a/kT) \ll 2n_{h0}.$$

On the other hand we get, by combining (18) and (23),

$$n_{h1}E_1 - (2n_{h0} - n_{h1})E_2 \approx -n_{hB}E_2 \exp(-eV_2/kT).$$

Neglecting the terms with n_{h1} on the left-hand side, we get

$$n_{hB} = 2n_{h0}\exp(eV_2/kT).$$

Since $(dV_2/dV_a)_q$ is negative according to (8), n_{hB} will decrease with increasing applied voltage. Thus, with a constant surface charge on the boundary, the electron concentration at the boundary increases while the hole concentration decreases with increasing applied voltage. The transition processes between the different energy levels will tend to increase the number of electrons on the boundary states.

Alternating-Current Admittance

The grain boundary can be represented by the equivalent circuit, Fig. 4, where Y_1 and Y_2 are the admittances for the conduction current and the C's are the capacitances of the barriers due to the variation of the space charge with the potential difference. We shall deal with Y's and C's per unit cross-section area of the specimen. These parameters are voltage dependent. We shall be interested in small ac voltages ($<kT/e$), when differential values can be used.

For zero dc bias, $Y_1 = Y_2 = Y_0$ and $C_1 = C_2 = C_0$ due to symmetry. Under this condition the conduction current as well as its separate components (electron and hole) are continuous throughout the grain boundary barrier. The electron current gives rise to a conductance given by (16). The hole current, however, gives as in the case of p–n junction, a complex admittance owing to the fact that outside the barrier it depends on recombination. Equation (21) and therefore (26) for the differential conductance at zero bias apply only in the dc case. For ac applied voltage, $\partial n_h/\partial t$ in (21) cannot be equated to zero. We have to use the solution in the form $n_h(x)\exp(j\omega t)$. Instead of (22), we then get

$$i_h = e(D_h/\tau)^{\frac{1}{2}}(1+j\omega\tau)^{\frac{1}{2}}(n_{hA} - n_{h0}). \quad (27)$$

Consequently the differential conductance at zero bias (26) becomes now a complex admittance:

$$Y_{h0} = G_{h0} + jB_0 = (e^2/2kT)(D_h/\tau)^{\frac{1}{2}}(1+j\omega\tau)^{\frac{1}{2}} n_{h0}. \quad (28)$$

The total admittance of the grain boundary at zero bias is

$$Y_0 = G_0 + jB_0 = G_{e0} + G_{h0} + j(B_{h0} + \omega C), \quad (29)$$

where C is the capacitance of the grain boundary, being C_1 and C_2 in series. B corresponds to an apparent capacitance B/ω, which is frequency dependent on

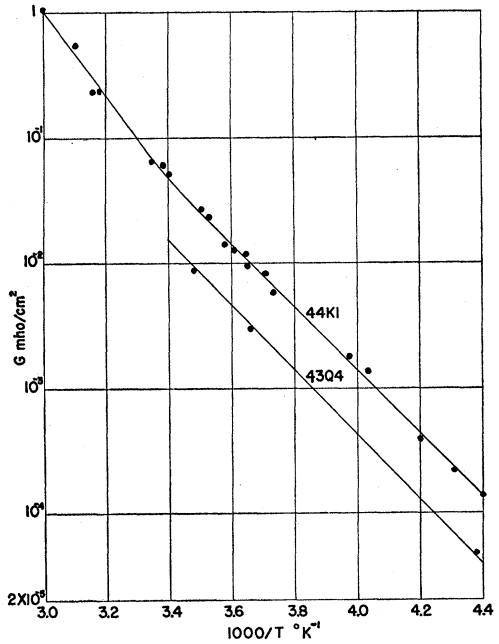

FIG. 6. Small-voltage conductance of two grain boundaries, samples 44K1 and 43Q4, as a function of reciprocal of temperature.

account of B_h. The hole concentration in the bulk material, n_{h0}, decreases rapidly with decreasing temperature. For sufficiently low temperatures, $\omega C \gg B_h$ and B/ω will be independent of frequency. It follows from (28) that $G_h > B_h$, the two approaching equality only at high frequencies. Therefore, if with decreasing temperature the conductance G should become very small compared to B, then the condition $\omega C \gg B_h$ must be fulfilled. Thus

$$B/\omega = C, \text{ if } G \ll B \text{ and } B/\omega \text{ is independent of frequency.} \quad (30)$$

Since the barrier resistance increases with applied voltage [Fig. 1, Eqs. (15) and (25)] when the effect of the conduction currents becomes negligible at zero bias, it must do so under applied bias also. It is therefore possible to study the dependence of the space charge capacitance on the applied bias at low temperatures.

EXPERIMENTAL RESULTS

Breakdown Voltage

For measurements with large voltages, pulses have to be used to avoid heating. Figure 5 shows a typical current-voltage characteristic of a grain boundary, measured with constant current square-wave pulses of 1 millisecond duration and 2 pulse per second repetition rate. The ohmic voltage drop in the bulk material is calculated from the resistivity and subtracted from the measured voltage to give the voltage drop across the grain boundary. The voltage wave shape is square, except where a dotted branch is shown. There the voltage decreases toward the end of the pulse, showing a decrease in the barrier resistance due to heating. The solid curve corresponds to the beginning, and the dotted branch corresponds to the end of the pulse. To make sure that heating effect had been eliminated, the curves were measured with 5-μsec and 2-μsec pulses.[11] The results agreed with the solid curves.

The breakdown voltage at which the current rises steeply is 84 volts in one direction and 115 volts in the other direction. Some dissymmetry is observed for all samples tested. This dissymmetry can be explained by a small difference between the impurity concentration on the two sides of the boundary. Even when there is no appreciable difference in the bulk resistivity on the two sides, it will still be possible to have a difference in the impurity concentration on the two sides of the boundary within the distance of the barrier thickness, 10^{-3} cm. As explained above, breakdown will occur if the surface charge does not increase any more with increasing applied voltage. We have pointed out that practically all of the applied voltage V_a is taken up by one of the potential barriers, while the potential drop across the other barrier remains close to its equilibrium value ϕ. With $V_a \gg \phi$ we get, according to (4),

$$q = -(\kappa e/2\pi)^{\frac{1}{2}}(NV_a)^{\frac{1}{2}}. \quad (31)$$

For $V_a = (V_1 - V_2) > 0$ we should use $N = N_1$, and for $V_a = (V_2 - V_1) > 0$ we should use $N = N_2$. It is clear that, for a given maximum value of q, the limits of the applied voltage for the two directions have the relation

$$V_{1\max}/V_{2\max} = N_2/N_1. \quad (32)$$

The experimental values of $V_{1\max}$ and $V_{2\max}$ for three samples are given in Table I. For sample 43Q4, the values of N_1 and N_2 have been determined by capacitance measurements and are given in Table III. Comparing column 6, Table I with column 4, Table III we see that $V_{2\max}/V_{1\max}$ agrees well with N_1/N_2. The maximum number of electrons on the boundary surface states, $n_{s\max} = -q/e$, as calculated according to (31), is given in column 7. The values of impurity concentration N used in this calculation is taken from Table III for sample 43Q4. For samples 44A2 and 44K1, the bulk impurity concentration given in column 3, Table I, and the average breakdown voltage for the two directions are used.

TABLE I. Breakdown measurements.

Sample	ρ ohm cm	n_{e0} cm^{-3}	$V_{1\max}$ volts	$V_{2\max}$ volts	$V_{2\max}/V_{1\max}$	$n_{s\max}$ cm^{-2}	$E_{\max}$ volt cm^{-1}
43Q4	3	7.0×10^{14}	84	115	1.37	1.08×10^{12}	1.2×10^{5}
44K1	4	5.2×10^{14}	108	145	1.34	1.08×10^{12}	1.2×10^{5}
44A2	15	1.5×10^{14}	133	158	1.18	0.62×10^{12}	0.7×10^{5}

[11] The authors are indebted to Dr. R. Bray for making these measurements.

McAffe, Ryder, Shockley, and Sparks[12] have shown that p–n junctions in germanium break down when the electric field in the barrier reaches about 2×10^5 volt-cm. The steep rise of current at the breakdown is attributed to the Zener current. The highest electric field occurs in our case at the boundary and is related to q according to (4):

$$q=-en_s\approx-\kappa E/4\pi.$$

The values of $E_{\max}$ at breakdown, calculated in this way, are given in the last column of Table I. The values for the three samples are consistently smaller than that given by the above authors for the onset of Zener current. However, the difference is not more than a factor of three and is perhaps not big enough to rule out definitely such a possibility.

Direct-Current Conductance

The conductance for small V_a due to the electron current is given by (16). All the samples tested have bulk resistivity of a few ohm-cm or higher. For such materials the mobility is determined primarily by lattice scattering and may be written as

$$\mu=bT^{-\frac{3}{2}},$$

where b is a constant. Equation (16) becomes

$$G_{e0}=K_eT^{-1}\exp[-(\phi+\zeta)/kT],$$

where

$$K_e=(e^2/2k)E_0A_eb_e. \tag{33}$$

Within the exhaustion range, a temperature range over which all the effective impurities are ionized, the concentration of electrons remains constant and the value of ζ varies almost linearly with temperature, according to the relation given by statistics:

$$\zeta=(kT/e)\ln(A_eT^{\frac{3}{2}}/n_e).$$

The value of the $(\phi+\zeta)$, Fig. 3, gives the position of the Fermi level ζ in the energy gap at the boundary, and consequently it determines the occupation of the surface states by electrons. On the other hand, ϕ is related to the space charge on the two sides of the boundary. The neutrality condition, i.e., that the magnitude of the positive space charge should be equal to the magnitude of the negative surface charge, determines ϕ. The space charge varies only slowly with ϕ, being proportional to $\phi^{\frac{1}{2}}$. If the density of surface states per unit energy is high, then a small change in $(\phi+\zeta)$ will result in a large change in the surface charge. Under such conditions $(\phi+\zeta)$ will remain practically constant, and ϕ will vary with ζ as the temperature changes. The curve $\ln G_{e0}$ *versus* $1/T$ should then be an approximately straight line, the slope of which gives $(\phi+\zeta)$. The constancy of $(\phi+\zeta)$ is born out by ac measurements reported later.

TABLE II. Dc conductance measurements.

Sample	ψ ev	$\phi+\zeta$ ev	K_e amp °K/volt cm²	K_e calculated amp °K/volt cm²
43Q4	0.515	0.535	0.7×10^{11}	3×10^{11}
44K1	0.495	0.517	1×10^{11}	$\sim3\times10^{11}$

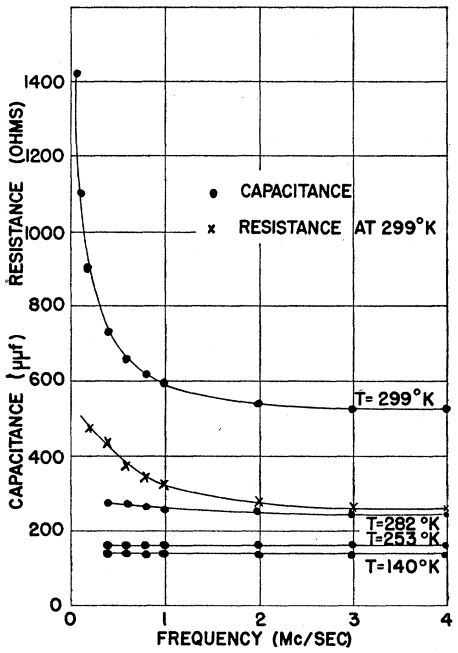

FIG. 7. Apparent capacitance and resistance of a grain boundary at different temperatures, as functions of frequency.

The conductance for small V_a due to the hole current is given by (26). We have the statistical relationship

$$n_en_h=4[2\pi(m_em_h)^{\frac{1}{2}}k/h^2]^3\,T^3\exp(-E_G/kT),$$

where E_G is the width of the forbidden energy gap. E_G may vary with temperature, and if it has a term linearly dependent on temperature, this term will have the effect of modifying the constant coefficient on the right-hand side. Experimentally it is found for germanium[13] that

$$n_en_h=\alpha T^3\exp(-E_{G0}/kT),$$

where

$$\alpha=8.5\times10^{31}\ \text{cm}^{-6}\ \text{°K}^{-3};\quad E_{G0}=0.73\ \text{ev}. \tag{34}$$

Since $D_h=\mu_hkT/e$, it follows from (26) and (34) that

$$G_{h0}=K_hT^{7/4}\exp(-E_{G0}/kT),$$

where

$$K_h=4.25\times10^{31}(e^3b_h/k\tau)^{\frac{1}{2}}n_{e0}^{-\frac{1}{2}}. \tag{35}$$

If τ does not vary very rapidly, the temperature dependence of G_{h0} will be predominately determined by the exponential factor. Similarly, the exponential factor

[12] McAfee, Ryder, Shockley, and Sparks, Phys. Rev. **83**, 650 (1951).

[13] V. A. Johnson and H. Y. Fan, Phys. Rev. **79**, 899 (1950).

in (33) controls the temperature variation of G_{e0}. Since $(\phi+\zeta)<E_{G0}$, we would expect G_{h0}/G_{e0} to increase with increasing temperature.

For the measurement of barrier conductance as a function of temperature, the samples were carefully cleaned, mounted in a tube, evacuated, and outgassed by repeated heating at about 400°C until reproducible results were obtained. This was necessary because at the grain boundary a high resistance is concentrated over a distance of the order 10^{-4} cm. It was also necessary to shield the tube from light, especially at the lower temperatures, since the grain boundary barriers are photoconductive. The measurements were made within the exhaustion range from −50°C to 60°C. For higher temperatures the semiconductor became intrinsic and the barrier resistance diminished rapidly. Figure 6 gives the results for two samples. Below 20°C the data can be fitted by an equation:

$$\ln G_0=\text{const}-\psi/kT.$$

The values of ψ are given in Table II. If the major part of the current were carried by holes, we should have $\psi\sim E_{G0}=0.73$ ev. Therefore, we conclude that the current in this temperature range is carried mainly by electrons with $\psi\sim(\phi+\zeta)$. To determine $(\phi+\zeta)$ and K_e of (33), the data were replotted with $\ln(G_0T)$ against $1/T$. The resulting curves have similar shapes to those shown in Fig. 6. The values of $(\phi+\zeta)$ and of K_e, obtained by straight line extrapolation to the axis $1/T=0$, are given in Table II for the two samples. For sample $44K1$ the measurements were carried to 60°C, just before entering the intrinsic range. We see in Fig. 6, that above 20°C the slope of the curve becomes steeper, indicating that hole current begins to be appreciable. These result support the point of view underlying our treatment. If there is an extensive region of p-type conduction at the grain boundary, so that the problem can be treated as p–n–p junctions, then the temperature dependence of both electron and hole currents will be determined essentially by[10] $\exp(-E_{G0}/kT)$, in contradiction with the experimental results.

A stringent test for the theory is the actual order of magnitude of the conductance. With a given value of $(\phi+\zeta)$, this means checking the value of the coefficient K_e. The last column in Table II gives the values calculated by using (33). The values of E_0 used are obtained from the barrier thickness L and barrier height ϕ_0 given in Table III. The calculated values of K_e and the experimental values are of the same order of magnitude. This can be considered to be very satisfactory. Furthermore, we have explained in connection with the curve for $44K1$, Fig. 6, that the larger slope at the high temperature end can be attributed to the hole current becoming appreciable. The bending begins at about $T=293$°K. According to the theoretical expression (35), for the hole current at this temperature to be 20 percent of the total measured current, τ should be around 200 μsec. This is a reasonable order of magnitude.

Capacitance

The impedance of such barriers at zero bias was measured as a function of temperature and frequency. Figure 7 shows the result for one sample. The apparent capacitance B/ω at room temperature is seen to depend strongly on frequency. The resistance $1/G$ also varies with frequency. As shown in (28) and (29), this is what we would expect if there is appreciable hole current through the barrier. Below 282°K the capacitance becomes independent of frequency and the conductance becomes much smaller than the susceptance, $G\ll B$ (by a factor of over 20, depending on the temperature). According to (30), the susceptance should give the actual space charge capacitance of the grain boundary consisting of two barriers in series. We have, by using (2), the capacitance of each barrier:

$$C=dQ/dV=(\kappa eN/8\pi V)^{\frac{1}{2}}. \tag{36}$$

As discussed before, under an applied voltage

$$V_a=(V_1-V_2)>0,$$

we have $V_1=V_a+\phi_1$, $V_2=\phi_2$. Thus, with a dc bias V_a, we get for the grain boundary

$$1/C=(8\pi/\kappa eN_1)^{\frac{1}{2}}[(V_a+\phi_1)^{\frac{1}{2}}+(\phi_2N_1/N_2)^{\frac{1}{2}}]. \tag{37}$$

The curves of Fig. 8 show C plotted *versus* $1/[(V_a+\phi)^{\frac{1}{2}}+\phi^{\frac{1}{2}}]$, where the parameter ϕ is chosen to give the best fit of the data by straight lines through the origin. According to (37) two parameters should be used, i.e., ϕ_1 and ϕ_2N_1/N_2 for one direction of the bias, and ϕ_2 and ϕ_1N_2/N_1 for the other direction. However, the right-hand side of (37) is not very sensitive to the parameter which appears as an additive term to V_a. Since N_2/N_1 is not very different from unity and the difference between ϕ_1 and ϕ_2 is small, a single parameter was adequate to give the desired fit. The value of ϕ so obtained is largely determined by the second term on the right of (37). Two such curves as given in Fig. 8 were obtained at each temperature, one for each direction of bias. From the slopes of these curves the

TABLE III. Capacitance measurements (Sample 43Q4).

T °K	N_1 cm^{-3}	N_2 cm^{-3}	N_1/N_2	ϕ' ev	ϕ'' ev	ϕ_0 ev	ζ ev	$\phi_0+\zeta$ ev	C_0 μμf	$C_0\phi_0^{\frac{1}{2}}$ μμf ev$^{\frac{1}{2}}$	L cm
271	8.5×10^{14}	6×10^{14}	1.4	0.35	0.24	0.29	0.23	0.52	147	79	1.7×10^{-4}
201	7.5×10^{14}	5×10^{14}	1.5	0.43	0.30	0.36	0.16	0.52	125	75	2.0×10^{-4}
103	8×10^{14}	6×10^{14}	1.3	0.51	0.39	0.44	0.08	0.52	120	79	2.1×10^{-4}

impurity concentrations N_1 and N_2 on the two sides of the boundary were determined according to (37), and these are given in Table III. The values obtained at different temperatures agree within experimental accuracy. The ratio N_2/N_1 is in fair agreement with the value given in Table I for the ratio of breakdown voltages $V_{1\max}/V_{2\max}$ for this sample, as prescribed by (32).

The two values of ϕ, ϕ' and ϕ'', used for the two straight lines of Fig. 8, should be $\phi''=\phi_1 N_2/N_1$ and $\phi'=\phi_2 N_1/N_2$. These values are given in Table III. Values are also given for

$$\phi_0=(\phi'\phi'')^{\frac{1}{2}}=(\phi_1\phi_2)^{\frac{1}{2}}.$$

The condition for equilibrium gives

$$\phi_2-\phi_1=\zeta_1-\zeta_2=kT\ln(n_{e2}/n_{e1})=kT\ln(N_2/N_1).$$

The last expression follows from complete ionization of the impurities. Thus the difference between ϕ_1 and ϕ_2 is small compared to either one of them, which is of the order of a fraction of 1 ev. Hence

$$\phi_0\approx\phi_1\approx\phi_2. \tag{38}$$

Table III shows that ϕ_0 varies with the temperature. The value of ζ calculated from the electron concentration in the bulk material is also given and it is seen that $(\phi+\zeta)$ remains constant for the various temperatures. This result confirms the discussions made in connection with the dc conductance measurements. The value of $(\phi_0+\zeta)$ agrees closely with the value in Table II for this sample.

The measured capacitance at zero bias C_0 is also given in Table III. According to (37) and (38), $C_0\phi_0^{\frac{1}{2}}$ should be a constant. The values for the three temperatures agree within the experimental accuracy. The total thickness of the grain boundary barrier L is, according to (36),

$$1/C=1/C_1+1/C_2=4\pi(l_1+l_2)/\kappa=4\pi L/\kappa. \tag{39}$$

The values of L at zero bias are given in the last column of Table III.

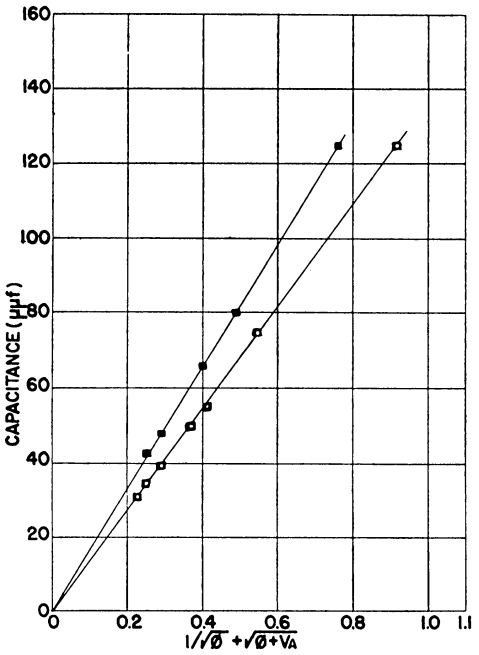

FIG. 8. Capacitance of a grain boundary for opposite polarities of applied bias V_a, at 201°K.

SUMMARY

The dc conductance G_{e0} of the grain boundary for sufficiently low temperatures agree with the theoretical expression (33) for the electron current. The capacitance measurements confirm the constancy of $(\phi+\zeta)$, the height of the barrier above the Fermi level. The values of $(\phi+\zeta)$ obtained from the capacitance measurements agree with the value estimated from the slope of the curve of $\ln(G_{e0}T)$ *versus* $1/T$. The increasing slope of this curve at the high temperature end and the large frequency dependence of the apparent capacitance at these temperatures are in agreement with the theory, and this indicates that the hole current should become more important with increasing temperature. Impurity concentrations on both sides of the grain boundary have been estimated from the measurements of capacitance as function of bias applied in both directions. A difference in the concentration is obtained; the ratio of the concentration agrees with the ratio of the breakdown voltages for the two directions. The maximum number of electrons on the boundary states, as calculated from the breakdown voltage, is of the order 10^{12} cm^{-2}. However, at the breakdown the electric field at the boundary approaches the field for the onset of Zener current, and it cannot be stated with certainty that the breakdown is caused by the saturation of the boundary states.